Towards Decentralized Parameter Servers for Secure Federated Learning

Muhammad El-Hindi, Zheguang Zhao and Carsten Binnig
Department of Computer Science, Technical University of Darmstadt, Germany

Keywords: Federated Learning, Privacy, Parameter Server, Decentralization, Sharding, Asynchronous Updates.

Abstract: Federated learning aims to protect the privacy of data owners in a collaborative machine learning setup since training data does not need to be revealed to any other participant involved in the training process. This is achieved by only requiring participants to share locally computed model updates (i.e., gradients), instead of the training data, with a centralized parameter server. However, recent papers have shown that privacy attacks exist which allow this server to reconstruct the training data of individual data owners only from the received gradients. To mitigate this attack, in this paper, we propose a new federated learning framework that decentralizes the parameter server. As part of this contribution, we investigate the configuration space of such a decentralized federated learning framework. Moreover, we propose three promising privacy-preserving techniques, namely model sharding, asynchronous updates and polling intervals for stale parameters. In our evaluation, we observe on different data sets that these techniques can effectively thwart the gradient-based reconstruction attacks on deep learning models, both from the client side and the server side, by reducing the attack results close to random noise.

1 INTRODUCTION

Motivation. Federated learning (FL) (McMahan et al., 2017) enables organizations to learn predictive models in a collaborative way. There are several reasons for using federated learning. One is that each individual organization has too little training data and thus data of multiple organizations is needed to train a deep model. Moreover, FL is interesting since the training data does not leave organizational boundaries (Kairouz et al., 2019; Li et al., 2020). This is especially helpful if the data contains private information that needs to be protected. A prime example for FL is healthcare. There, multiple hospitals want to learn a model over their joint data for the classification of a new disease, but need to keep patient data local due to legal and privacy regulations (Brisimi et al., 2018).

The predominant architecture for federated learning today is to use a central parameter server (PS) that collects the model updates from all participants and aggregates them. In this setup, the data owners participate in the training process by sending their locally computed model updates to the central server, which combines these updates into a global model (McMahan et al., 2017). The original assumption was that such an approach is able to protect the privacy of each participant's training data, since only model updates and not the training data itself is exchanged with the server. Yet, recent works (Zhu et al., 2019; Zhao et al., 2020) have shown that privacy attacks exist that allow an attacker to successfully extract information about the training data by observing the model updates (i.e., exchanged gradients). More surprisingly, these attacks showed that it is possible to successfully reconstruct individual training examples with high accuracy (e.g., a full picture used for training) (Zhu et al., 2019; Zhao et al., 2020). Even worse, these attacks are also applicable for different model architectures (Geiping et al., 2020; Wei et al., 2020).

Meanwhile existing defense strategies remain limited in preventing privacy attacks in federated learning (Zhu et al., 2019; Geiping et al., 2020; Phong et al., 2018; Bonawitz et al., 2017; Abadi et al., 2016). Most strategies either significantly reduce the learning accuracy (e.g., using noisy gradients can result in 30% less accuracy (Zhu et al., 2019)) or have other limitations such as assuming a trusted central PS, or being incompatible with widely used model architectures (e.g., secure aggregation (Bonawitz et al., 2017)). Generic cryptographic primitives such as homomorphic encryption, although not affecting accuracy, typically incur significant overhead resulting in longer training times (e.g., by 100x (Phong et al., 2018)).

Contributions. In this work we take a different, system-driven approach by modifying the federated learning framework. We propose to ar-

El-Hindi, M., Zhao, Z. and Binnig, C.
Towards Decentralized Parameter Servers for Secure Federated Learning.
DOI: 10.5220/0011146300003269
In *Proceedings of the 11th International Conference on Data Science, Technology and Applications (DATA 2022)*, pages 257-269
ISBN: 978-989-758-583-8; ISSN: 2184-285X

chitect the training system around decentralize parameter servers. Further, we initiate the study of the configuration space of such a decentralized FL framework, called `P2Sharding`, w.r.t. its security against client-side and server-side attacks. We propose three promising privacy-preserving techniques, namely model sharding, asynchronous updates and polling intervals on stale parameters. Our evaluation on the CIFAR10 and MNIST datasets shows that these configurations can effectively thwart the gradient-based reconstruction attacks on deep learning models by reducing the attack outcome close to random noise.

Outline. The remainder of this paper is organized as follows. Section 2 gives an overview of federated learning and the common basis for existing privacy attacks. We present our privacy-preserving sharding framework based on a decentralized parameter server architecture in Section 3. We evaluate these configurations in Section 4 and conclude with related work and a summary.

2 BACKGROUND

In the following, we briefly discuss the basics of federated learning and the typical structure of privacy attacks on federated learning. Finally, we review existing defense strategies when using a central parameter server and their limitations.

2.1 Federated Learning

Federated learning is a collaborative learning setting in which multiple parties jointly train a machine learning model. To coordinate the learning process, federated learning typically uses a central parameter server to initialize a global model, and interacts with a set of participants (clients) to collect updates to the model. One distinct aspect of this setting is that participants never upload their data to the server, and the only information the server collects is model updates computed on privately held data (McMahan et al., 2017; Kairouz et al., 2019; Bonawitz et al., 2019). The de facto class of training algorithms deployed in the federated setting for deep learning is stochastic gradient descent (SGD). SGD updates are gradients of model weights towards minimizing a loss function computed on batches of the training data (Konečný et al., 2016). Training data is possibly iterated through multiple times locally before sending the final update to be averaged to the server (McMahan et al., 2017). The parameter server aggregates

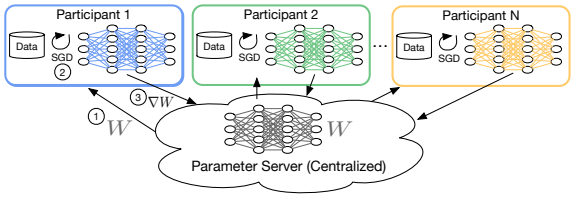

Figure 1: Federated learning with a centralized parameter server using stochastic gradient descent (SGD). Each participant ① downloads global model parameters W from the server; ② computes local model updates ∇W based on privately held data; ③ sends local updates to the server. The server aggregates the local updates to global parameters.

updates from each client, and applies changes to the model parameters either synchronously (Chen et al., 2017) (accepting one update per client in a round) or asynchronously (Dean et al., 2012) (allowing clients to progress independently).

Figure 1 illustrates the basic steps. Each client k downloads the parameters W, computes the gradient $\nabla_W L(W; x_k, y_k)$ for the loss function L on its local data (x_k, y_k) (denoted as $\nabla W(x_k, y_k)$) . The server collects each gradient and aggregates it into the global model $W \leftarrow W - \eta \sum_{k=1}^{K} \beta_k \nabla W(x_k, y_k)$ with the weights β_k and the learning rate η. The interactive process iterates until convergence.

2.2 Privacy Attacks

Since its inception, federated learning has emerged as a common paradigm to train on real-world privacy sensitive data. It was commonly believed that the information transmitted over the network in federated settings contains only minimal updates for improving the model, and therefore reveals much less information about the private training data (Konečný et al., 2016; McMahan et al., 2017). However, this conceived advantage has been cast into doubt by recent work on privacy attacks that revealed that even the model updates contain enough information to compromise the data privacy (Melis et al., 2018; Zhu et al., 2019; Geiping et al., 2020).

The authors (Melis et al., 2018) show that gradients carry valuable information that can be leveraged by attackers to leak unintended knowledge about the private data. The authors of (Zhu et al., 2019) were the first to show that it is even possible to reconstruct full images and text data with high precision from gradients sent by clients and thus breach the privacy of the learning process. This class of reconstruction attacks only requires access to the exposed model updates (i.e., the gradients ∇W), plus the parameters W and is therefore applicable to most federated settings.

The common basis for these attacks is the following optimization problem: Find some estimated data

x' (e.g., an image) and its label y' (e.g., the classification of the image) such that its gradient $\nabla_W L(x', y')$ is closest to the transmitted client gradient ∇W for its private input x and label y. In other words, the distance of the two gradients with regard to a distance function $\mathbb{D}()$ is minimized:

$$\arg\min_{x',y'} \mathbb{D}\big(\nabla W, \nabla_W L(W, x', y')\big) \tag{1}$$

The original attack (Zhu et al., 2019) used an L-BFGS solver (Liu and Nocedal, 1989) with randomly initialized (x', y') to optimize Eq. (1) based on the euclidean distance for a training batch size of 1. The attack accuracy was improved by (Zhao et al., 2020) in which the private labels y are recovered analytically from the direction of the gradients. More recently, (Geiping et al., 2020) used cosine similarity in Eq. (1) to yield a stronger attack for larger batch sizes.

2.3 Existing Defense Strategies

The key ingredients for the reconstruction attacks in Eq. (1) are: (a) the access to the entire model parameters W, and (b) the view of the entire gradient ∇W. Several countermeasures based on differential privacy (Zhu et al., 2019), gradient compression (Lin et al., 2018; Zhu et al., 2019) and cryptography (Bonawitz et al., 2017; Phong et al., 2018) were proposed. Yet, they have several limitations:

Differential Privacy Approach. The differential privacy-based approach in (Zhu et al., 2019) adds Lapacian and Gaussian noise to the local model updates before transmission, but larger noise is often necessary for enough privacy protection, which tends to degrade the training accuracy significantly.

ML-based Approach. Gradient compression (Lin et al., 2018) by dropping out small gradient components has shown to be effective only when the sparsity of the gradient exceeds 20% (Zhu et al., 2019). Yet, this method does not prevent a corrupt server from inverting the gradients from observed model iterates, a crucial step for reconstruction (cf. Sec. 3.2.2).

Cryptographic Approach. Some cryptographic protocols are still ineffective against the attack in (Geiping et al., 2020), e.g., secure aggregation (Bonawitz et al., 2017) or, in the case of Homomorphic encryption (Phong et al., 2018), incur prohibitive overhead and are limited to integer fields. A multi-party computation-based approach (Goldreich, 1998) also has large overhead when scaling to more than two servers or clients or is not directly applicable to the federated setting as is the case for the approach in (Mohassel and Zhang, 2017).

3 DECENTRALIZED SECURE FL

In the following, we present an alternative, system-driven approach for enhancing privacy in federated learning without the drawbacks seen in the above mentioned approaches. We first give an overview of our decentralized parameter server that partitions the model into shards. We then discuss how these model shards are created and updated on different server instances in order to enhance data privacy.

3.1 Decentralized Parameter Server

Centralized parameter server presents a single point of security vulnerability because a corrupt server can see all updates from all clients and launch the gradient-based reconstruction attack as is. By contrast, we proposed to base our defense mechanism on decentralizing the parameter server.

Instead of congregating the model parameters on a centralized PS, our framework, called `P2Sharding`, distributes trust among several independent parameter server instances, each hosting a fraction of the model, called a *shard*. No single server instance holds the entire model W, nor receives the entire gradient ∇W. Thus just by design, sharding enhances data privacy by preventing the adversary from having a consistent view of the entire gradients and the model parameters, both the key elements in the reconstruction attacks.

Federated Settings. We consider a set of K clients who participate to train a model on their joint data. The model W is partitioned into M shards $W^1, \cdots, W^M$ using a configurable strategy, and each shard W^m is hosted on a separate parameter server instance. Each server instance W^m receives the gradient shard ∇W^m from each client k. Each client downloads the full model iterates $W = (W^1, \cdots, W^M)$ by sending requests (i.e., polling) to the M server instances.

Note that the amount of exchanged data between clients and the parameter server shards is similar to the classical central parameter server setting. In both cases, clients need to download the full model W or send all gradients ∇W to a remote location. The only additional overhead introduced by our framework are additional messages/connections since clients have to communicate with multiple remote endpoints.

The framework can adapt to several federated settings using different configurations. For example, for enterprise clients where each has enough computation resource, each of the M server instances can be co-located with a client. An example is shown in Figure 2. In contrast, a server-aided model can be used to outsource the M server instances onto M independent

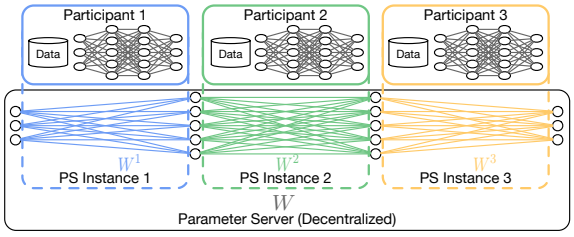

Figure 2: Decentralized Parameter Server Architecture for an example with 3 shards (W^1, W^2, W^3). *The parameter space W is partitioned across several independent PS instances managed by different participants. In the example, the PS instances are co-located with each participant, but they can also be hosted by independent physical servers.*

physical servers, which is more suitable for resource-constrained clients running on edge devices such as mobile phones.

Security Model. The `P2Sharding` framework assumes all parties to be *semi-honest*, that is each client and server follow their prescribed protocol and only attempts to extract more information from the other client's data[1]. Moreover, at least one client and one shard are assumed to be non-colluding with the other parties (i.e., we have at least two non-colluding shards). Otherwise, the security reduces to that of a centralized server.

We also consider cases where (1) a subset of PS instances or (2) client and server instances collude (e.g., due to being co-located as shown in Figure 2). In the first case, the goal of the colluding PSs is to extend their knowledge about exchanged gradients. In the second case, the attacker only wants to get access to the full model iterates $W^1, \cdots, W^M$ since the client regularly receives the latest global model. This provides crucial information for reconstruction because the attacker can estimate the full gradients from the *history* of the received model iterates.

In `P2Sharding`, we provide several configurations to help reduce the risk of both PS-side and client-side attacks as explained next.

3.2 Privacy-preserving Configurations

We turn to investigate several configurations within the `P2Sharding` framework that can enhance privacy. These configurations are rooted in system designs, and therefore present a different tool for protecting private training data than differential privacy or end-to-end cryptographic approaches.

[1]Protocols that assume a semi-honest setup prevent inadvertent leakage of information between parties, and are thus useful if this is the concern. In addition, protocols in the semi-honest model are quite efficient, and are often an important first step for achieving higher levels of security.

3.2.1 Model Sharding

Since a shard contains only a partition of the model, the information leakage to a corrupt server is limited to its hosted shard. Which data can be reconstructed from a shard depends on how the model parameters are distributed. For example, if the penultimate layer in a feed-forward, softmax-output neural network were allocated to the same shard, its corrupt server may learn the training label (Zhao et al., 2020). In the following, we describe three sharding strategies that provide strong privacy in our evaluation, and we show how to vary the shard size to increase resilience against collusion of multiple shards.

Uniform Sharding. The idea of the *Uniform*-strategy is to create S similar-sized shards that store the same fraction of parameters from each layer, as depicted in Figure 3. As shown in the figure, all three shards have the same size and equally span all layers.

In order to achieve this partitioning, the strategy uniformly assigns the parameters p_i to the shards W^j. This can be expressed by selecting a shard for a parameter at index i using a shared hash function $\mathcal{P}$:

$$\mathcal{S}(i) = \big(\mathcal{P}(i) \bmod S\big) + 1 \tag{2}$$

Uniform sharding creates equally-sized partitions. However, it is completely oblivious of the different layers and hence a participant might possess parameters from all layers.

Slicing Sharding. Another model-oblivious technique is the *Slicing*-strategy. In this strategy, the parameter space is contiguously divided into S equally-sized partitions, as depicted in Figure 3. More formally, this strategy can be described by the following function:

$$\mathcal{S}(i) = \left\lceil \frac{i}{\frac{|W|}{S}} \right\rceil \tag{3}$$

Intuitively, we can linearly iterate over all parameters in W and assign the first $\frac{1}{S}$ parameters to the first shard (blue) and the second $\frac{1}{S}$ to the second (green) shard and so on.

In terms of shard size, this strategy creates equally sized shards as shown in Figure 3.Moreover, shards span only a few layers of a NN as depicted in the example. There, the blue and yellow shard span multiple layers but the green shard is limited to a single parameter-layer. Hence, this strategy differs from the *Uniform*-strategy since it reduces the number of layers from which a participant holds parameters.

Boundary-aware Sharding. In contrast to the previous strategies, this strategy guarantees that a partition does not hold any parameters of adjacent

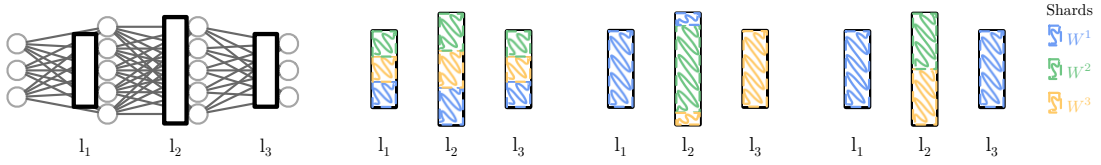

(a) Layers of model parameters. (b) Uniform. (c) Slicing. (d) Boundary-aware.

Figure 3: *Partitioning Strategies for a neural network (NN) model architecture with four layers (a); i.e., three layers of parameters since the input layer has no parameters. (b) The* Uniform *strategy creates equally sized partitions that span across all layers. (c) The* Slicing *strategy divides the parameters into equally sized consecutive slices (only some of which span layers). (d) The* Boundary-aware *strategy guarantees that while a shard may posses parameters from multiple layers, these layers are not adjacent. This strategy might create shards of different sizes.*

parameter-layers, e.g., the blue shard in Figure 3 does not hold any parameters from layer l_2. Further, this strategy might create partitions with a different number of parameters in order to prevent a shard from storing parameters from adjacent layers. This situation can be seen in Figure 3 since the blue shard is bigger than the remaining two shards.

Such a mapping can be expressed as follows:

$$\mathscr{S}(i,l) = \begin{cases} (\mathscr{P}(i) \bmod \lfloor \frac{S}{2} \rfloor) + 1, & l \bmod 2 = 1 \\ (\mathscr{P}(i) \bmod \lceil \frac{S}{2} \rceil) + \lceil \frac{S}{2} \rceil, & l \bmod 2 = 0 \end{cases} \tag{4}$$

That is, we distinguish two sets of shards, one is responsible for odd layers ($l \bmod 2 == 1$) while the other stores the parameters of the even layers ($l \bmod 2 == 0$). We create these two sets by splitting the shards in two halves ($\lfloor \frac{S}{2} \rfloor$). For example, we can observe in Figure 3 that shard W^1 is responsible for the odd layers, while shard W^2 and W^3 are responsible for the even layer. Moreover, within every set of shards, the parameters are uniformly distributed with the help of a uniform shared hash function $\mathscr{P}(i)$. Note that, we have decided to assign more shards to the even layers (i.e., using $\lfloor \rfloor$ as first bound), since even layers tend to contain more parameters (cf. Figure 3) than, e.g., the odd in-/output layers. While the *Boundary-aware*-strategy does not create equally-sized partitions, it takes the layer boundaries of the model architecture into account and avoids that shards receive gradients of two adjacent layers.

Shard Sizes. The `P2Sharding` framework provides the shard size configuration parameter for adjusting the privacy of sharding in light of collusion attacks. The effect of a collusion attack is the same as if several shards were combined to form a larger subset of the model. Hence, the shard size is privacy-sensitive in that it can be used to control for the expected number of collusions. Intuitively, if C server instances collude, their knowledge is the union of their shards. If the number of colluding shards becomes large enough the reconstruction attack becomes easier. So by reducing the maximum shard size S, `P2Sharding` can control the amount of leakage during C shard-collusion to be $\leq C \cdot S$ gradient components.

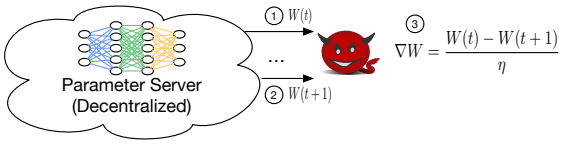

Figure 4: Attackers recovering full gradients from model iterates. *The estimation takes three steps: Downloading all parameters from all shards repeatedly (① and ②) and assembling the global model at t and $t+1$. Finally, both models are used to recompute the gradients that were used to update W_t to W_{t+1} ③. For the Stochastic Gradient Descent (SGD) algorithm, the gradients can be recomputed with the shown formula.*

3.2.2 Asynchronous Updates

This configuration aims to reduce the risk of malicious client and server collusion.

Leakage from Synchronous Updates. Under synchronous training, with the help of a colluding server, a malicious client can retrieve model snapshots of different iterations for a targeted victim, then uncover the full gradient to launch the gradient-based attack. As depicted in Figure 4 an attacker could continuously retrieve (i.e., poll) the latest model from all parameter servers to determine $W(t)$ ① and $W(t+1)$ ② and re-compute the gradients ∇W based on the retrieved models ③. This observation especially holds true for standard SGD which uses the update rule $W(t+1) = W(t) - \eta * \nabla W$ with learning rate η (i.e. $\nabla W = \frac{W(t)-W(t+1)}{\eta}$) for computing the new model parameters. In other SGD variants, gradients may only be estimated from the full history of model iterates $\{W(t)\}_t$.

Perturbation by Asynchronous Updates. Our approach to mitigate the aforementioned gradient recovery is to use *asynchronous federated updates*. In this setting, concurrent client updates to the same model

shard are applied without a global order, which may lead to the effect of different clients overwriting each other's model updates, or some clients update some shards more often than others. As a result, data reconstruction becomes harder as shown in our evaluation.

Intuitively, if multiple updates to each shard are incorporated asynchronously in parallel, then the full model iterates may contain out-of-sync values. This leads to non-uniform directional perturbation in the estimated full gradients. Following the model iterate analysis for asynchronous SGD (Mania et al., 2017), such perturbation can be modeled as essentially injecting random noises $\mathcal{E}(t)$ on the model iterates to the adversary's view g:

$$\nabla\widehat{W} = g\big(\{W(t)+\mathcal{E}(t)\}_t\big) \tag{5}$$

where $\mathcal{E}(t)$ is a vector that describes perturbation per shard j at time t. Thus the attacker only sees a gradient with noisy rotation and stretch. Since it is the angle of the gradient that contains most information about the data (Geiping et al., 2020), our evaluation shows that perturbed gradients indeed make data reconstruction harder while maintaining model accuracy high.

3.2.3 Polling Intervals

Asynchronous updates can lead to degraded model quality for some models and datasets (Mania et al., 2017). For these cases where asynchronous updates are not applicable, we introduce *polling intervals* as another means to perturb model iterates for privacy. The idea is to create stale parameters, while still allowing for *synchronous* updates to the entire model for more stable training.

More specifically, each server instance j can independently implement a manual random delay τ_j, called the polling interval, for each connecting client. For each request, the server instance checks the client's identity, and answers with an outdated model shard $W^j(t-\tau_j)$. All such artificially out-of-sync model shards form a client's view on the entire model, which crucially still contains inconsistent values at all time. As such this setting can also resist the reconstruction attack. Specifically, the difference between the latest but hidden model shard $W^j(t)$ and the polled model shard $W^j(t-\tau_j)$ can be viewed as the source for the perturbation $\mathcal{E}(t)$ in Eq. (5) at a particular time t. As such, polling intervals provide a deterministic way for inducing perturbation through staleness.

An important point to note here is that each parameter server instance is assigned to a separate trust domain with its internal states hidden from the environment, that is, it only exposes its interface to the other parties. Hence, each PS instance can actually implement different strategies of which data can be read from the local shard. That way, each server instance in `P2Sharding` can control parameter staleness local to its shard by keeping track of the updated model versions (i.e., one version per iteration) and return a model with a definable staleness to the client.

Finally, another interesting observation is that model iterates with the same increasing polling interval actually also produce a similar effect of increasing the batch size, since it results in accumulated updates across multiple training examples. As shown in (Zhu et al., 2019) and in (Geiping et al., 2020) an increased batch size makes privacy attacks harder. We validated the effectiveness of polling interval in Section 4 for both privacy and performance.

4 EXPERIMENTS

Overall the goal of the evaluation is to analyze the effects of the different configurations of `P2Sharding` on privacy protection. We first demonstrate that the privacy of the training data can be significantly strengthened with the help of `P2Sharding`'s decentralized setting when compared to a centralized parameter server. We then decompose `P2Sharding` into each of its configurations. We show that for varying data and model complexities `P2Sharding` is able to provide configurations under which the attack results remained unrecognizable, i.e., close to random noise.

4.1 Setup and Metrics

In our evaluation we used a similar setup as the original reconstruction attack (Zhu et al., 2019; Geiping et al., 2020), because our goal is to show that the range of configurations in `P2Sharding` can mitigate such attacks successfully. More details on the setup are provided below:

Dataset Complexities. We used the `MNIST` (LeCun, 1998) and `CIFAR10` (Krizhevsky, 2009) datasets as representatives for less and more complex datasets. `MNIST` is considered less complex than `CIFAR10` for it contains only black-and-white images of handwritten digits, whereas `CIFAR10` contains colored images of more complex objects.

Model Complexities. As models, we used `LeNetZhu` as in (Zhu et al., 2019) and `ConvNet` as in (Geiping et al., 2020) to represent lower and higher model complexities. Both models are widely-used convolutional neural networks. However, one noticeable difference is their depth, or number of layers, since `ConvNet` is deeper than `LeNetZhu`.

Another important difference from a reconstruction attack perspective is the used activation function. LeNetZhu uses a Sigmoid function which makes the network inherently twice-differentiable, resulting in a smoother optimization problem in attack formulation (Eq. 1). ConvNet by contrast uses ReLU which is non-smooth and non-differentiable at 0.

Attack Implementation. For the attacks, we used the code in (Geiping et al., 2020) (cosine similarity based reconstruction attack) and adapted their hyper-parameters for the actual learning process (i.e., SGD with learning rate $\eta = 0.1$). We integrated our partitioning strategies by implementing a separate module that limits the gradients that are accessible to the attacker (i.e., a PS instance).

In the following, we always execute 5 attacks on randomly selected training batches. Thereby, we set the batch size to 1, as done in (Zhu et al., 2019), since this represents the worst-case that P2Sharding has to defend against — as mentioned in (Zhu et al., 2019), a bigger batch size makes the attack harder. Further, we executed each experiment three times.

Privacy Metrics. In order to evaluate the privacy against reconstruction attacks, we measured the *structural dissimilarity* (DSSIM) of a reconstructed image from its targeted private image. The DSSIM is derived from the *structural similarity* (SSIM) (Wang et al., 2004) as $DSSIM(x,y) = \frac{1-SSIM(x,y)}{2}$. We used this measure instead of the *mean squared error* (MSE) as in (Zhu et al., 2019) or the MSE-based peak noise-to-signal ratio as in (Geiping et al., 2020), because DSSIM not only captures pixel-local deviation but more importantly the structural differences. Hence, it has been shown to be a superior measure for signal fidelity such as perceptual distortion or *recognizability* (Brunet et al., 2012). For example, a color-inverted MNIST image (a black-and-white digit) will have extremely high MSE, but it does not correlate with the privacy of the image as the structure of the digit remains obviously the same. In contrast, the DSSIM value for the same image will be kept low to reflect the structural similarity. In general, a higher DSSIM suggests the reconstructed image deviates more from the private image and may even be unrecognizable. We show a sample of images from MNIST and CIFAR10 with varying DSSIM in Figure 5. Three reconstructed images were randomly selected to represent different DSSIM intervals. It can be observed that when the DSSIM reaches a value > 0.45 the reconstruction become unrecognizable, which coincides with the DSSIM of random noise.

In our evaluation, we recorded the empirical distribution of DSSIM over MNIST and CIFAR10 under repeated attacks, and reported the average and minimum DSSIM as average and worst-case performance.

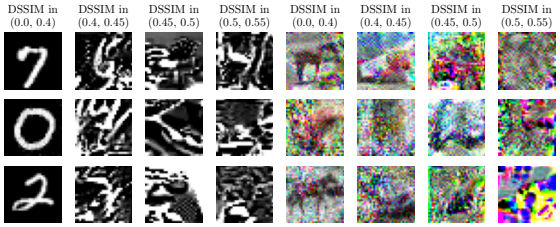

Figure 5: Visualization of different DSSIM ranges for attacks on the MNIST (left) and CIFAR10 (right) dataset. *A higher* DSSIM *value means that an attack was unsuccessful and privacy is protected. For* MNIST *and* CIFAR10 *privacy is protected beginning with a* DSSIM > 0.45.

Baselines. In the following we compared P2Sharding to two baselines. As the first baseline, we compared against a centralized parameter server with no sharding. This setting represents an insecure setup and we show that P2Sharding configurations achieve much stronger privacy. This baseline will be shown as red dashed line in the experiment plots. On the other hand, the best privacy against reconstruction is to have attack results close to random noise. Hence, we also compared against a randomly generated picture in which each pixel is sampled i.i.d. from a uniform range (shown as a green dotted line in the following figures).

4.2 Decentralized vs. Centralized PS

In the first experiment we evaluate the privacy gain from sharding the model parameters in the decentralized parameter server setting, as compared to the centralized parameter server without sharding.

To that end, we used P2Sharding to partition the parameter space using the three proposed sharding techniques. Additionally, we varied the number of shards used to partition the model parameters in order to capture the effect of varying shard sizes ($size = \frac{1}{\#shards}$). For instance, a shard size of 0.5 refers to the fact that the model was split into 2 partitions. We then randomly selected a resulting partition and measured the DSSIM when executing reconstruction attacks across all datasets and model architectures.

The results of this experiment can be seen in Figure 6. All sharding techniques show a clear improvement over the centralized parameter server baseline (dashed red line). In particular, the benefit of sharding is most visible when looking at the success of the best attack (called worst-case scenario) in Figure 6. Without sharding the centralized setting is consistently able to recover some private image. However, with P2Sharding we were able to find config-

urations (e.g., shard size = 0.12) that result in DSSIM values close to random noise even in the worst-case.

While Figure 6 illustrates that all partitioning strategies improve privacy clearly when compared to the baseline without sharding, it also reveals subtle differences among the different strategies, i.e., not all strategies get close to the upper bound of a random picture (green dotted line) for all settings. In the following, we analyze these difference in more detail.

4.3 Effects of Model Sharding

P2Sharding provides configurations for different sharding strategies. Each sharding strategy determines which parameters are stored in the same shard. Since an attacker sees at least one shard of gradients, it is important to understand the privacy impact of different ways of sharding. In the following, we shed more light on when to use which sharding strategy.

In Figure 6, we compared the three proposed sharding strategies across data and model characteristics. The first important observation is that the attack becomes consistently harder on more complex datasets (i.e., CIFAR10 bottom row). This observation is in line with what was reported in previous work (Zhao et al., 2020; Geiping et al., 2020). Therefore, we mainly used the simpler MNIST dataset to differentiate the privacy impact of the sharding strategies.

In the case of the MNIST data (upper row) we make the following observations. For the simple LeNetZhu model, both the uniform and the boundary-aware strategy result in lower DSSIM values than the slicing sharding technique. This can be observed in terms of both the average (Figure 6) and the worst-case performance (Figure 6). With decreasing shard size (ie., higher number of shards) both strategies improve and eventually achieve similar or slightly better (in terms of the worst-case) privacy protection than the slicing strategy.

For the more complex ConvNet model, the opposite effect is noticeable: Initially the uniform and the boundary-aware strategy show a better (worst-case) performance than the slicing strategy (see Figure 7). Yet, with decreasing shard size again all strategies provide comparable performance.

We found that this effect can be explained by the boundary-awareness of the different strategies, as will be outlined next.

Figure 7 reveals two key observations: First, limiting the gradients of a shard to only one layer yields (as in the slicing strategy) a relatively consistent performance across different shard sizes. Secondly, in the case of the MNIST dataset the last layer (Layer-3) enables more successful attacks (lower DSSIM) even for smaller shard sizes (e.g., 0.06). This is the case for both average as well as the worst-case performance shown in Figure 7. For the ConvNet model, however, this effect is not as significant and is only partially observable in the worst-case performance.

This experiment highlights that different layers of a deep learning model can carry more information than others. Further, and even more importantly, limiting the information of a shard to one layer provides a more robust privacy protection compared to the uniform and boundary-aware strategy (Figure 6).

Yet, as shown next, the ability of P2Sharding to control the shard size helps to improve the privacy protection of sharding strategies.

4.3.1 Reducing Shard Sizes

The main idea of the P2Sharding framework is to partition the global model into several shards hosted on independent parameter server instances. Intuitively, with smaller shard sizes a corrupted parameter server learns less about the gradients of the model, which increases the resistance to data reconstruction.

To evaluate this concept, we used the uniform strategy to create shards of different sizes and measure the success of reconstruction attacks for different model complexities on the MNIST dataset. We used the uniform strategy, since out of the three proposed strategies it had the most sensitivity to changing shard sizes. Hence, using this setup we show that reducing the shard size is another effective measure to make the privacy for sharding more robust.

Figure 8 shows the result of this experiment for various shard sizes on the x-axis. We can see, that by reducing the shard size the privacy protection is improved significantly. Starting from a shard size below 0.12, P2Sharding is able to achieve a privacy protection that was otherwise only reached by boundary-aware sharding.

4.4 Effects of Asynchronous Updates

If P2Sharding is used for asynchronous updates the different parameter shards can be updated at different points in time. In general, with more clients concurrently training and updating the model shards, the more staleness on average one can observe, and the larger such variance across shards becomes (Mania et al., 2017).

In the experiment shown in Figure 9, we simulated the effect of concurrent activities and stale shards (i.e., delayed parameter updates) by randomly delaying the incorporation of an update in a shard. We studied the effects of staleness with no additional polling (i.e., polling interval = 1) and with a high polling interval.

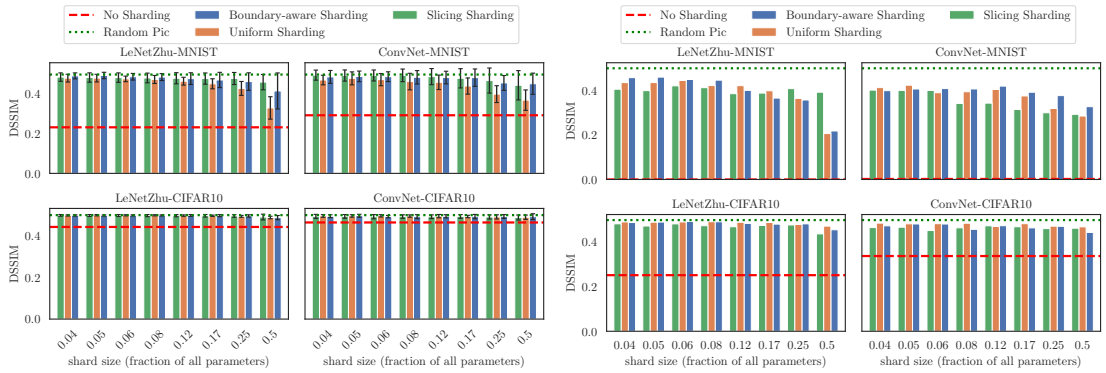

(a) Average Performance (b) Worst-case Performance

Figure 6: Evaluation of the proposed sharding techniques in terms of (a) the average success and (b) the success of the best attack (called worst-case scenario). *All sharding techniques show a clear improvement over the baseline (dashed red line).*

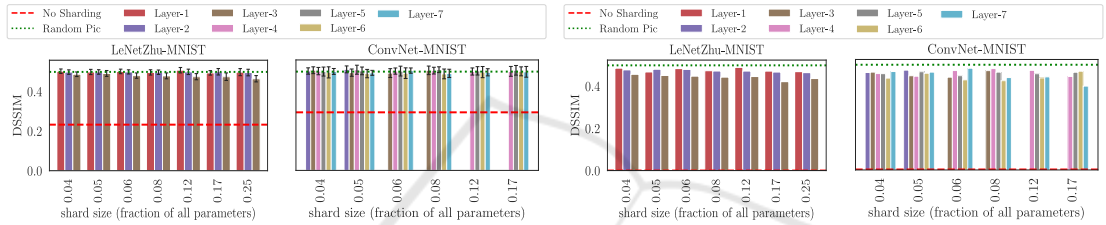

(a) Average Performance (b) Worst-case Performance

Figure 7: Relative Importance of Layers. An attack based on the later layers of a model seem to have a higher chance for a successful attack (lower DSSIM value). This effect is most noticeable for simple data as well as models and when looking at the worst-case performance (Figure 7).

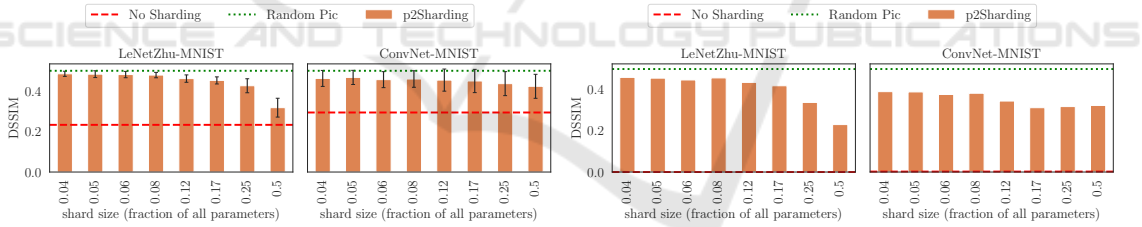

(a) Average Performance (b) Worst case Performance

Figure 8: Influence of the shard size on privacy attacks (zoom-in into Figure 6). *Decreasing the shard size is an effective measure to prevent attacks. This is shown by the increasing* DSSIM *(less successful attack) for small shard sizes (e.g.,* 0.12*).*

In our setup, already with an average staleness per shard increased to 2, we observed that all data and models started to have increased resistance to reconstruction. That is, the average DSSIM (Figure 9) increases. With more concurrency, such as when the average staleness reached 8, the privacy becomes close to the ideal privacy of random noise, even for a simple model and dataset. This effect was even stronger when a polling interval of 8 was used in addition, which suggests that polling intervals contribute significantly towards an increased privacy protection. Hence, we will study the effect of polling intervals in more detail in the next section.

4.5 Effects of Polling Intervals

Similar to asynchronous updates, polling intervals aim at preventing client-side attacker from uncovering the full gradient, a crucial step in reconstruction. However, polling intervals rely on serving parameters with randomly varying staleness to perturbe the attacker's view on the entire model. The added benefit is that polling intervals can work with synchronous updates to all the model shards such that the training becomes more stable.

In the experiment of Figure 10, we observed that with increasing polling intervals, the resistance to

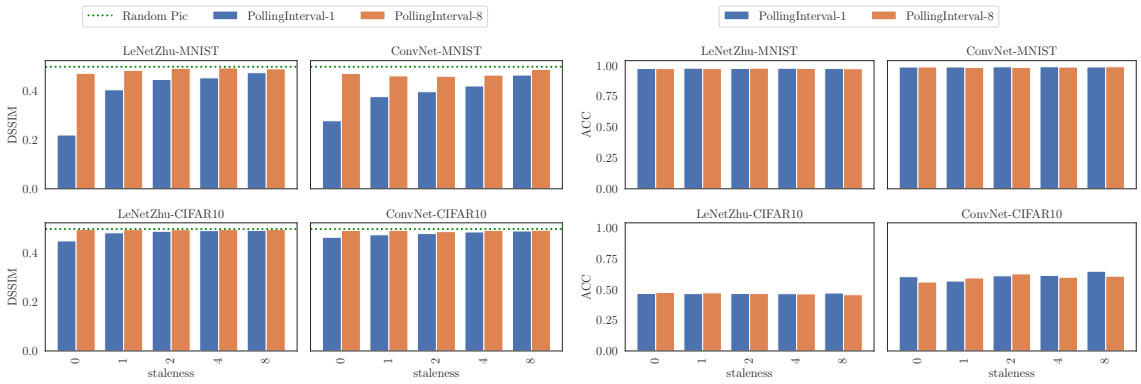

(a) Average Performance

(b) Accuracy

Figure 9: Influence of staleness on privacy attacks. Staleness makes the model iterates inconsistent across all shards as in a typical asynchronous learning setup since the shards incorporate client updates with a delay. An increased staleness helps to improve the privacy protection, i.e., increase the DSSIM (9) while not affecting the resulting model accuracy (9).

construction also became stronger. This effect was most obvious when the staleness due to asynchronous updates was controlled for and set to 0 (i.e., no staleness created by asynchronous updates, blue bar). We note that this setting is essentially polling interval combined with *synchronous updates*. With the only effect left due to polling intervals, we observed that a higher average interval at 8 consistently achieved higher resistance to attacks than without the polling interval (i.e., 1) across all data and model complexities (cf. Figure 10).

On a final note, in both experiments of the asynchronous training and polling intervals we observed consistently high test accuracy as reported in Figure 9 and Figure 10. This finding is consistent with previous work on asynchronous learning that showed that asynchronous updates achieve robust training quality (Dean et al., 2012; Mania et al., 2017).

5 RELATED WORK

Privacy Preserving Machine Learning. While Federated Machine Learning represents a recent technique to protect the privacy of training data, preserving the privacy in machine learning is a much broader area of research (Shokri and Shmatikov, 2015; Abadi et al., 2016; Mohassel and Zhang, 2017; Bonawitz et al., 2017; Phong et al., 2017; Phong et al., 2018). In particular, (Mohassel and Zhang, 2017) considers a non-federated setting where users upload secret shares of their data on two non-colluding servers. (Shokri and Shmatikov, 2015) uses a central parameter server to host the up-to-date model. It allows clients to train on the latest model while only sending selective gradients. However, it cannot prevent gradient-based attacks from colluding clients or a corrupt server.

Privacy in Federated Machine Learning (ML). There have already been several existing approaches for enhancing privacy in Federated ML. In fact, cryptographic techniques such as differential privacy (McMahan et al., 2018), homomorphic encryption (Liu et al., 2020) or secure multi-party computation (Bonawitz et al., 2017) have also been proposed to improve the privacy in the context of federated learning. However, as mentioned previously these techniques show several limitations such as limited compatibility with different model architectures or an increased learning overhead.

Recently, papers also explored non-cryptographic techniques to protect privacy in Federated ML, such as gradient compression (Lin et al., 2018; Zhu et al., 2019). In this technique, gradients with small values are pruned to zero such that the number of useful gradients that are sent to the server are limited. While this technique also limits the amount of information available to an attacker, it depends heavily on whether gradients can be pruned or not and can influence the training process negatively.

Decentralized Architectures and Sharding. Moreover, there has been a lot of work in the context of decentralized machine learning (Lian et al., 2017; Ormándi et al., 2013). This works mainly focus on how to enable ML without using any central (parameter) server component. In contrast, our approach does not eliminate the parameter server, but decentralizes this component itself. The most similar approach with this regard is the work in (El-Mhamdi et al., 2020). However, compared to their architecture, which assumes a full replication of parameters across

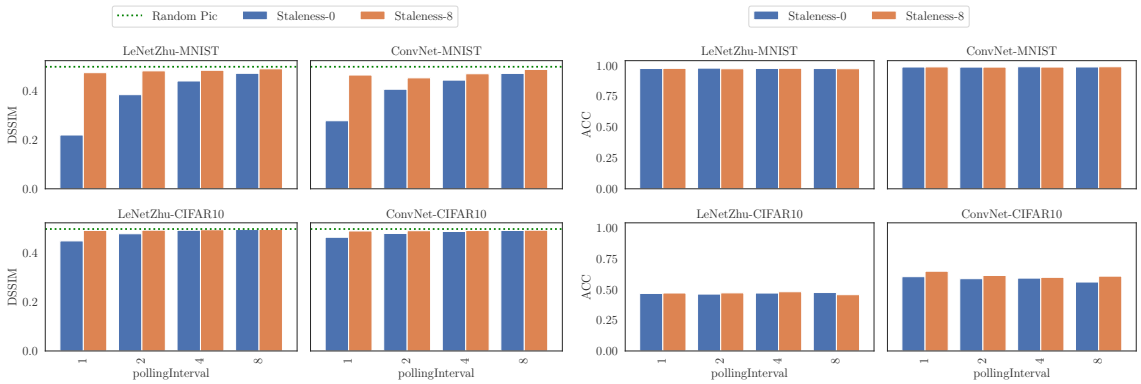

(a) Average Performance

(b) Accuracy

Figure 10: Influence of polling intervals on privacy attacks. Polling intervals enable `P2Sharding` to introduce asynchronous effects even to synchronous training. As for staleness, an increased polling interval improves the privacy protection, i.e., increases the `DSSIM` (10) while not affecting the resulting model accuracy (10).

all server instances to make the overall training robust against potentially misbehaving parameter servers and thus to tolerate Byzantine failures, our approach utilizes sharding to distribute parameters across server instances to achieve privacy.

Lastly, sharding or partitioning in general has widely been used in both database systems (DeWitt and Gray, 1992) and ML systems (Dean et al., 2012; Chilimbi et al., 2014; Li et al., 2014; Xing et al., 2015) to improve scalability and performance or reduce communication costs (Zhang et al., 2020). However, to the best of our knowledge, looking at sharding from a privacy perspective is a new proposal.

6 CONCLUSION AND FUTURE WORK

The security of federated learning was recently called into question by works on gradient-based attacks to reconstruct private trainnig data. In this work, we initiated the study of secure FL based on a different, decentralized parameter server architecture called `P2Sharding`. We proposed three configurations on how to partition, serve and update the model parameters for better privacy. Empirical evidence on CIFAR10 and MNIST showed noticeably stronger resilience against gradient-based data reconstruction attacks by limiting the attack outcome close to random noise. In future work, we aim to further establish the formal security analysis of our FL framework.

Several areas for other future work exist. Our framework can be extended with differential privacy or cryptographic tools to further strengthen the security such as against malicious adversaries or support secure synchronous non-stochastic optimization. Another work is to develop an automatic mechanism to optimally configure our framework given a wider range of models and datasets. Lastly our framework may also be extended for other security concerns in federated learning such as data and model poisoning.

ACKNOWLEDGEMENTS

This work was partially funded by the National Research Center ATHENE, the BMWK project SafeFBDC (01MK21002K), and the BMBF project TrustDBle (16KIS1267). We also thank hessian.AI for the support.

REFERENCES

Abadi, M., Chu, A., Goodfellow, I. J., McMahan, H. B., Mironov, I., Talwar, K., and Zhang, L. (2016). Deep learning with differential privacy. In Weippl, E. R., Katzenbeisser, S., Kruegel, C., Myers, A. C., and Halevi, S., editors, *ACM SIGSAC, CCS 2016*, pages 308–318, Vienna, Austria. ACM.

Bonawitz, K., Eichner, H., Grieskamp, W., Huba, D., Ingerman, A., Ivanov, V., Kiddon, C., Konecný, J., Mazzocchi, S., McMahan, B., Overveldt, T. V., Petrou, D., Ramage, D., and Roselander, J. (2019). Towards federated learning at scale: System design. In Talwalkar, A., Smith, V., and Zaharia, M., editors, *MLSys 2019*, pages 374–388, Stanford, CA, USA. mlsys.org.

Bonawitz, K. A., Ivanov, V., Kreuter, B., Marcedone, A., McMahan, H. B., Patel, S., Ramage, D., Segal, A., and Seth, K. (2017). Practical secure aggregation for privacy-preserving machine learning. In Thuraisingham, B. M., Evans, D., Malkin, T., and Xu, D., editors, *ACM SIGSAC, CCS 2017*, pages 1175–1191, Dallas, TX, USA. ACM.

Brisimi, T. S., Chen, R., Mela, T., Olshevsky, A., Paschalidis, I. C., and Shi, W. (2018). Federated learning of predictive models from federated electronic health records. *Int. J. Medical Informatics*, 112:59–67.

Brunet, D., Vrscay, E. R., and Wang, Z. (2012). On the Mathematical Properties of the Structural Similarity Index. *IEEE Transactions on Image Processing*, 21(4):1488–1499.

Chen, J., Pan, X., Monga, R., Bengio, S., and Jozefowicz, R. (2017). Revisiting distributed synchronous sgd. *arXiv*, pages 1–10.

Chilimbi, T. M., Suzue, Y., Apacible, J., and Kalyanaraman, K. (2014). Project adam: Building an efficient and scalable deep learning training system. In Flinn, J. and Levy, H., editors, *OSDI 2014*, pages 571–582, Broomfield, CO, USA. USENIX Association.

Dean, J., Corrado, G., Monga, R., Chen, K., Devin, M., Le, Q. V., Mao, M. Z., Ranzato, M., Senior, A. W., Tucker, P. A., Yang, K., and Ng, A. Y. (2012). Large scale distributed deep networks. In Bartlett, P. L., Pereira, F. C. N., Burges, C. J. C., Bottou, L., and Weinberger, K. Q., editors, *NIPS 2012*, pages 1232–1240, Lake Tahoe, NV, USA. Curran Associates, Inc.

DeWitt, D. J. and Gray, J. (1992). Parallel database systems: The future of high performance database systems. *Commun. ACM*, 35(6):85–98.

El-Mhamdi, E., Guerraoui, R., Guirguis, A., Hoang, L. N., and Rouault, S. (2020). Genuinely distributed byzantine machine learning. In Emek, Y. and Cachin, C., editors, *ACM PODC 2020, Virtual Event*, pages 355–364, Italy. ACM.

Geiping, J., Bauermeister, H., Dröge, H., and Moeller, M. (2020). Inverting gradients - how easy is it to break privacy in federated learning? In Larochelle, H., Ranzato, M., Hadsell, R., Balcan, M., and Lin, H., editors, *NeurIPS 2020, 2020, virtual*.

Goldreich, O. (1998). Secure multi-party computation. *Manuscript. Preliminary version*, 78.

Kairouz, P., McMahan, H. B., Avent, B., Bellet, A., Bennis, M., Bhagoji, A. N., Bonawitz, K. A., Charles, Z., Cormode, G., Cummings, R., D'Oliveira, R. G. L., Rouayheb, S. E., Evans, D., Gardner, J., Garrett, Z., Gascón, A., Ghazi, B., Gibbons, P. B., Gruteser, M., Harchaoui, Z., He, C., He, L., Huo, Z., Hutchinson, B., Hsu, J., Jaggi, M., Javidi, T., Joshi, G., Khodak, M., Konečný, J., Korolova, A., Koushanfar, F., Koyejo, S., Lepoint, T., Liu, Y., Mittal, P., Mohri, M., Nock, R., Özgür, A., Pagh, R., Raykova, M., Qi, H., Ramage, D., Raskar, R., Song, D., Song, W., Stich, S. U., Sun, Z., Suresh, A. T., Tramèr, F., Vepakomma, P., Wang, J., Xiong, L., Xu, Z., Yang, Q., Yu, F. X., Yu, H., and Zhao, S. (2019). Advances and open problems in federated learning.

Konečný, J., McMahan, H. B., Yu, F. X., Richtárik, P., Suresh, A. T., and Bacon, D. (2016). Federated Learning: Strategies for Improving Communication Efficiency. pages 1–10.

Krizhevsky, A. (2009). Learning multiple layers of features from tiny images. Technical report, University of Toronto.

LeCun, Y. (1998). The mnist database of handwritten digits.

Li, M., Andersen, D. G., Park, J. W., Smola, A. J., Ahmed, A., Josifovski, V., Long, J., Shekita, E. J., and Su, B. (2014). Scaling distributed machine learning with the parameter server. In Flinn, J. and Levy, H., editors, *OSDI 2014*, pages 583–598, Broomfield, CO, USA. USENIX Association.

Li, T., Sahu, A. K., Talwalkar, A., and Smith, V. (2020). Federated learning: Challenges, methods, and future directions. *IEEE Signal Process. Mag.*, 37(3):50–60.

Lian, X., Zhang, C., Zhang, H., Hsieh, C., Zhang, W., and Liu, J. (2017). Can decentralized algorithms outperform centralized algorithms? A case study for decentralized parallel stochastic gradient descent. In Guyon, I., von Luxburg, U., Bengio, S., Wallach, H. M., Fergus, R., Vishwanathan, S. V. N., and Garnett, R., editors, *NIPS 2017*, pages 5330–5340, Long Beach, CA, USA.

Lin, Y., Han, S., Mao, H., Wang, Y., and Dally, B. (2018). Deep gradient compression: Reducing the communication bandwidth for distributed training. In *ICLR 2018*, Vancouver, BC, Canada. OpenReview.net.

Liu, D. C. and Nocedal, J. (1989). On the limited memory BFGS method for large scale optimization. *Math. Program.*, 45(1-3):503–528.

Liu, Y., Kang, Y., Xing, C., Chen, T., and Yang, Q. (2020). A secure federated transfer learning framework. *IEEE Intelligent Systems*, 35(4):70–82.

Mania, H., Pan, X., Papailiopoulos, D., Recht, B., Ramchandran, K., and Jordan, M. I. (2017). Perturbed iterate analysis for asynchronous stochastic optimization. *SIAM Journal on Optimization*, 27(4):2202–2229.

McMahan, B., Moore, E., Ramage, D., Hampson, S., and y Arcas, B. A. (2017). Communication-efficient learning of deep networks from decentralized data. In Singh, A. and Zhu, X. J., editors, *AISTATS 2017*, pages 1273–1282, Fort Lauderdale, FL, USA. PMLR.

McMahan, H. B., Ramage, D., Talwar, K., and Zhang, L. (2018). Learning differentially private recurrent language models. In *ICLR 2018*, Vancouver, BC, Canada. OpenReview.net.

Melis, L., Song, C., Cristofaro, E. D., and Shmatikov, V. (2018). Inference attacks against collaborative learning. *CoRR*, abs/1805.04049:1–16.

Mohassel, P. and Zhang, Y. (2017). SecureML: A System for Scalable Privacy-Preserving Machine Learning. In *IEEE SP 2017*, pages 19–38, San Francisco, CA, USA. ISSN: 2375-1207.

Ormándi, R., Hegedüs, I., and Jelasity, M. (2013). Gossip learning with linear models on fully distributed data. *Concurr. Comput. Pract. Exp.*, 25(4):556–571.

Phong, L. T., Aono, Y., Hayashi, T., Wang, L., and Moriai, S. (2017). Privacy-Preserving Deep Learning: Revisited and Enhanced. In Batten, L., Kim, D. S., Zhang, X., and Li, G., editors, *Applications and Techniques in Information Security*, Communications in Computer and Information Science, pages 100–110, Singapore. Springer.

Phong, L. T., Aono, Y., Hayashi, T., Wang, L., and Moriai, S. (2018). Privacy-Preserving Deep Learn-

ing via Additively Homomorphic Encryption. *IEEE Transactions on Information Forensics and Security*, 13(5):1333–1345.

Shokri, R. and Shmatikov, V. (2015). Privacy-Preserving Deep Learning. In *ACM SIGSAC,CCS 2015*, pages 1310–1321, Denver, Colorado, USA. ACM Press.

Wang, Z., Bovik, A. C., Sheikh, H. R., and Simoncelli, E. P. (2004). Image quality assessment: from error visibility to structural similarity. *IEEE Trans. Image Process.*, 13(4):600–612.

Wei, W., Liu, L., Loper, M., Chow, K. H., Gursoy, M. E., Truex, S., and Wu, Y. (2020). A framework for evaluating gradient leakage attacks in federated learning. *CoRR*, abs/2004.10397:1–25.

Xing, E. P., Ho, Q., Dai, W., Kim, J. K., Wei, J., Lee, S., Zheng, X., Xie, P., Kumar, A., and Yu, Y. (2015). Petuum: A new platform for distributed machine learning on big data. In Cao, L., Zhang, C., Joachims, T., Webb, G. I., Margineantu, D. D., and Williams, G., editors, *ACM SIGKDD 2015*, pages 1335–1344, Sydney, NSW, Australia. ACM.

Zhang, Z., Wu, W., Jiang, J., Yu, L., Cui, B., and Zhang, C. (2020). Columnsgd: A column-oriented framework for distributed stochastic gradient descent. In *IEEE ICDE 2020*, pages 1513–1524. IEEE.

Zhao, B., Mopuri, K. R., and Bilen, H. (2020). idlg: Improved deep leakage from gradients. *CoRR*, abs/2001.02610:1–5.

Zhu, L., Liu, Z., and Han, S. (2019). Deep leakage from gradients. In Wallach, H. M., Larochelle, H., Beygelzimer, A., d'Alché-Buc, F., Fox, E. B., and Garnett, R., editors, *NeurIPS 2019*, pages 14747–14756, Vancouver, BC, Canada. Curran Associates, Inc.